Published in final edited form as:
Cancer Res. 2005 May 1; 65(9): 3883–3893.

The Synergistic Combination of the Farnesyl Transferase Inhibitor Lonafarnib and Paclitaxel Enhances Tubulin Acetylation and Requires a Functional Tubulin Deacetylase

Adam I. Marcus[1], **Jun Zhou**[1], **Aurora O'Brate**[1], **Ernest Hamel**[2], **Jason Wong**[3], **Michael Nivens**[1], **Adel El-Naggar**[4], **Tso-Pang Yao**[5], **Fadlo R. Khuri**[1], and **Paraskevi Giannakakou**[1]

[1]*Winship Cancer Institute, Emory University School of Medicine, Atlanta, Georgia* [2]*Screening Technologies Branch, Developmental Therapeutic Program, Division of Cancer Treatment and Diagnosis, National Cancer Institute, NIH, Frederick, Maryland* [3]*Harvard University, Cambridge, Massachusetts* [4]*The University of Texas M.D. Anderson Cancer Center, Houston, Texas* [5]*Department of Pharmacology and Cancer Biology, Duke University, Durham, North Carolina*

Abstract

Farnesyl transferase (FT) inhibitors (FTI) are anticancer agents developed to target oncogenic Ras proteins by inhibiting Ras farnesylation. FTIs potently synergize with paclitaxel and other microtubule-stabilizing drugs; however, the mechanistic basis underlying this synergistic interaction remains elusive. Here we show that the FTI lonafarnib affects the microtubule cytoskeleton resulting in microtubule bundle formation, increased microtubule stabilization and acetylation, and suppression of microtubule dynamics. Notably, treatment with the combination of low doses of lonafarnib with paclitaxel markedly enhanced tubulin acetylation (a marker of microtubule stability) as compared with either drug alone. This synergistic effect correlated with FT inhibition and was accompanied by a synergistic increase in mitotic arrest and cell death. Mechanistically, we show that the combination of lonafarnib and paclitaxel inhibits the *in vitro* deacetylating activity of the only known tubulin deacetylase, histone deacetylase 6 (HDAC6). In addition, the lonafarnib/taxane combination is synergistic only in cells lines expressing the wild-type HDAC6, but not a catalytic-mutant HDAC6, revealing that functional HDAC6 is required for the synergy of lonafarnib with taxanes. Furthermore, tubacin, a specific HDAC6 inhibitor, synergistically enhanced tubulin acetylation in combination with paclitaxel, similar to the combination of lonafarnib and paclitaxel. Taken together, these data suggest a relationship between FT inhibition, HDAC6 function, and cell death, providing insight into the putative molecular basis of the lonafarnib/taxane synergistic antiproliferative combination.

Introduction

Farnesyl transferase (FT) inhibitors (FTI) are a novel class of antineoplastic agents that have high antitumor activity and are currently in clinical trials (1–3). These agents inhibit the FT enzyme, which posttranslationally modifies proteins by the addition of a 15-carbon farnesyl group. The initial driving force behind FTI development was based on the finding that oncogenic Ras, a low molecular weight GTPase, induces malignant transformation upon addition of a farnesyl group to its COOH terminus by the FTase. This in turn allows it to localize

Requests for reprints: Paraskevi Giannakakou Winship Cancer Institute, Emory University School of Medicine, Room D4054, 1365C Clifton Road, Atlanta, GA 30322. E-mail: pgianna@emory.edu..

Note: Supplementary data for this article are available at Cancer Research Online (http://cancerres.aacrjournals.org/).

to the plasma membrane and acts as a relay switch by transducing biological information from extracellular signals to the nucleus (for review see ref. 4).

Because Ras farnesylation is required for Ras membrane localization, FTase became an attractive target for new anticancer agents (5–7). Furthermore, based on the finding that oncogenic Ras mutations are found in 30% of all human cancers (8,9), it was hypothesized that tumor growth could be inhibited by preventing Ras farnesylation. Thus, FTIs were developed as targeted agents against Ras and were shown to inhibit Ras function (10) as well as possess potent antitumor activity in multiple cancer cell lines and animal models. Despite the initial hypothesis that FTIs inhibit tumor growth by inhibiting Ras farnesylation, it was later shown that FTIs show antitumor activity independent of Ras status (11–13), suggesting that the mechanism of FTI activity extends beyond the inhibition of Ras farnesylation (14).

To probe the molecular mechanisms of FTI action, some previous works have focused on the relationship between FTIs and microtubule-targeting agents. Microtubules are dynamic polymers composed of α - and β -tubulin subunits that elongate and shorten. In the cell, they function in a variety of processes including cell division, cell signaling, and intracellular trafficking (reviewed in ref. 15). Because microtubules are essential components of the cell division machinery, they are attractive and validated targets for anticancer therapy (16,17) as evidenced by the clinical success of microtubule-targeting drugs such as taxanes (18–20). More recently, epothilones, a new class of microtubule-targeting drugs, are in clinical development and show very positive preliminary results (21). Notably, FTIs in combination with paclitaxel or epotholines act synergistically to inhibit cell growth in numerous human cancer cell lines and xenograft models (14,22–24). In addition, a combination clinical study of the FTI lonafarnib (SCH66336 or sarasar) with paclitaxel yielded impressive preliminary results, with partial responses in 8 of 20 evaluable patients, including patients whose disease had previously progressed while on taxanes alone (25). Despite these promising results, the molecular mechanism of the synergistic interaction of FTIs with taxanes is unknown.

The synergy between taxanes and FTIs suggests that there may be a link between microtubules and the mechanism of FTI action. This is further supported by studies showing that FTI-2153 inhibited normal bipolar microtubule spindle formation, suggesting that spindle microtubules may have been affected by this treatment (26–28). These FTI-treated cells were arrested in early mitosis and this effect was independent of p53 and Ras status. Nevertheless, the effects of FTI treatment on interphase microtubules have not been examined.

Here we investigated the effects of lonafarnib (29) on interphase microtubules in lung and breast cancer cells. Our results show that exposure to lonafarnib resulted in microtubule bundle formation, stabilized interphase microtubules, and suppressed microtubule dynamics. Moreover, we show that the combination of lonafarnib and paclitaxel for 16 hours synergistically enhanced tubulin acetylation, mitotic arrest, and cell death; furthermore, this effect correlated with FT inhibition. In addition, the combination of lonafarnib and paclitaxel inhibits the deacetylating activity of histone deacetylase 6 (HDAC6) *in vitro*, whereas either drug alone does not. Importantly, we show that the lonafarnib/taxane combination is synergistic only in cells lines expressing the wild-type HDAC6, but not a catalytic-mutant HDAC6, revealing that functional HDAC6 is required for the synergy of lonafarnib with taxanes. Taken together, these data suggest a relationship between FT inhibition, HDAC6 function, enhanced tubulin acetylation, and cell death, providing a putative molecular basis for the lonafarnib/taxane antiproliferative combination.

Materials and Methods

Cell culture

The human non–small cell lung cancer cell lines A549 and H1299 were maintained in RPMI 1640 supplemented with 5 % FCS, nonessential amino acids, and 0.1% penicillin/streptomycin at 37° C in 5% CO_2. Live cell microscopy was done with MCF-7 breast cancer cells stably transfected with green fluorescent protein (GFP):α -tubulin and maintained in DMEM supplemented with 5% FCS, nonessential amino acids, and 0.1% penicillin/streptomycin.. All lines were cultured at 37° C in a humidified atmosphere with 5 % CO_2. N IH-3T3 cells expressing various HDAC6 constructs were previously generated (30) and were cultured in DMEM medium under the same conditions.

Immunofluorescence analysis

Immunofluorescence microscopy was done as previously described (31). Cells were fixed in PHEMO buffer (68 mmol/L PIPES, 25 mmol/L HEPES, 15 mmol/L EGTA, 3 mmol/L $MgCl_2$, 10% DMSO) with 3.7% formaldehyde, 0.05% glutaraldehyde, and 0.5% Triton X-100. Cells were washed in PBS thrice for 5 minutes then blocked in 10% goat serum for 15 minutes. The following primary antibodies were used: α -tubulin (Chemicon International, Temecula, CA; 1:500 dilution) and acetylated tubulin (Sigma, St. Louis, MO; 1:1,000 dilution) with incubation time of 1 hour. The secondary antibodies used were Alexa 563–conjugated goat anti-rat immunoglobulin G (IgG; 1:500) and Alexa 488–conjugated goat anti-mouse IgG antibody (1:500), both from Molecular Probes (Eugene, OR). Cells were imaged using a Zeiss LSM 510 Meta (Thornwood, NY) confocal microscope using a either a 63 × [numerical aperture (NA) = 1.4] or 100× (NA = 1.4) Apochromat objective. To stain DNA for mitotic cell counting, we fixed cells as described above, and added Sytox Green (Molecular Probes) to the Gel Mount mounting media (Biomeda Corp., Foster City, CA). All images were acquired using Zeiss LSM 510 software and processed in Adobe Photoshop 7.0.

Cell tubulin polymerization assay

Quantitative drug-induced tubulin polymerization was done as previously described (32,33). The percent pellet (%P) is calculated as the amount of polymerized tubulin (P) over the total amount of polymerized and soluble tubulin (P + S) times 100 {%P = [P/(P + S)] × 100} based on densitometric analysis.

Electron microscopy

A549 cells were seeded on Thermanox coverslips (Electron Microscopy Sciences, Hatfield, PA) in 24-well plates and grown overnight to 60% confluency. Cells were then treated with 10 − mol/L lonafarnib for 48 hours and fixed using a protocol described in Vanier et al. (34). Cells were then fixed in 2% glutaraldehyde for 4 hours at room temperature, rinsed in distilled water twice, postfixed in 1% OsO_4 in 0.1 mol/L sodium cacodylate buffer (pH 7.4) at 4 ° C for 1 hour, and finally rinsed in distilled water as above. Samples were then dehydrated through an ethanol series (30%, 50%, 60%, 80%, 90%, 100%) followed by two changes of propylene oxide (10 minutes each). Then samples were infiltrated with Embed 812 (Electron Microscopy Science) for 3 days according to the instructions of the manufacturer. Each block was cut at 1 × 1 mm using a diamond knife and RMC MT-7000 ultramicrotome, and thin sections were made and collected onto 200 mesh copper grids. Grids were poststained with 10% uranyl acetate in distilled water and then 2% lead citrate in distilled water for 20 minutes in each treatment.

Flow cytometry analysis

To determine acetylated tubulin levels, cells were plated and on the following day treated with different concentrations of the drugs for 16 hours. After drug treatment, cells were fixed with PHEMO buffer for 10 minutes as previously described (31) and stained with an antibody against acetylated tubulin (Sigma; 1:500) followed by secondary Alexa 488–conjugated goat anti-mouse IgG antibody (1:500). Finally, cells were scraped into 1 mL of PBS, and flow cytometry analysis was done on a Becton Dickinson flow cytometer.

For cell cycle analysis, cells were scraped from plates, centrifuged at 1,000 rpm for 5 minutes, and propidium iodide buffer containing 0.1 mg/mL propidium iodide and NP40 (0.6%) in water was used to resuspend cells. Cell were incubated in this buffer for 30 minutes at room temperature in the dark, then passed through a filter to remove cell clumps, and finally read in a Becton Dickinson flow cytometer.

Microtubule dynamics assays

Experiments were done using a MCF-7 breast cancer cell line stably expressing a GFP-α -tubulin microtubule reporter protein (kind gift of Dr. Mary Ann Jordan). Cells were plated and analyzed as previously described (35). Images were taken using a Hamamatsu Orca ER camera (Middlesex, NJ) every 4 seconds for 2 minutes (250-400 seconds of exposure) on a Zeiss Axiovert epifluorescence microscope equipped with 100× Apochromat (NA = 1.4) oil lens and adjustable mercury arc lamp (set at 100% intensity). A stage heater as well as Zeiss heating chamber was used to maintain the temperature at 37 ± 0.5° C. Microtubules ends at the lamellar edge of interphase cells were imaged and subsequently tracked using the ‘‘track points’’ feature on Metamorph image analysis software (Universal Imaging, Downingtown, PA). The coordinates generated from this tracking feature were used to determine the distance individual microtubule ends changed from a fixed point. These values were transferred to a Microsoft Excel spreadsheet and used to generate life history plots of individual microtubules. From these graphs, the various variables shown in Table 1 were calculated. All *P* values were calculated using the Student’s *t* test.

Microtubule dynamicity is defined as the total length grown and shortened during the life (measured in minutes) of an individual microtubule. A catastrophe is defined as a transition into microtubule shortening whereas a rescue is a transition from shortening to growth or pause. To calculate catastrophe frequency per unit time or per unit length, the number of catastrophes was divided by the total time in growth and pause or the total distance grown, respectively. Conversely, the rescue frequency was calculated by dividing the number of rescues by the total time spent shortening or distance shortened.

In vitro acetylated tubulin assay

A549 cells were transiently trans-fected with Flag-tagged pBJ5-HDAC6 expression plasmids using FuGene (Roche, Basel, Switzerland) following the guidelines of the manufacturer. Untransfected cells or cells transfected with an empty vector were used as controls. In Fig. 5*A*, we used NIH-3T3 cells stably expressing FLAG-tagged HDAC6-wt and HDAC6-mt proteins and therefore cells did not have to be transfected. Cell lysates were prepared 48 hours after transfection and then immunoprecipitated with anti-Flag M2 agarose beads (Sigma). Tubulin acetylation assays were done by incubating the immunoprecipitates with preformed mitogen-activated protein–stabilized microtubules at 37° C, along with the appropriate drug, for 2 hours as described previously (30). Reactions were then placed on ice for 15 minutes and centrifuged briefly at 14,000 rpm to separate the supernatant from the agarose beads. The supernatant was analyzed by Western blotting with antibodies against acetylated α -tubulin and against α -tubulin (as described below) and the beads were analyzed with an antibody against Flag M2 (Sigma; 1:1,000).

Western blotting

Cells were plated in six-well plates at 50% confluency and treated the next day with the appropriate drug and time interval. Cells were lysed, centrifuged at 15,000 rpm for 15 minutes, and electrophoresed on a 7.5% SDS-PAGE gel (bicinchoninic acid assay was used to determine protein concentration in a spectrophotometer). Proteins were transferred to a polyvinylidene difluoride membrane (100 V for 1 hour) using a Bio-Rad transfer apparatus and blotted with antibodies against acetylated tubulin (Sigma; 1:1,000), total tubulin (Sigma DM1α ; 1:1,000), HDJ-2, acetylated histone 3 (Cell Signaling, Beverly, MA; 1:1,000), actin, and HDAC6 (Cell Signaling; 1:1,000).

Cell survival and synergy assays (combination index analysis)

Cells were plated in a 96-well plate at 2,000 cells/well and allowed to attach overnight. Cells were then treated with serial dilutions (1:3) of either lonafarnib alone, paclitaxel alone, or the combination of lonafarnib and paclitaxel for 72 hours. Cell were then fixed with 10% trichloroacetic acid for 30 minutes, washed thrice with water, dried, and stained with 0.4% sulfurhodamine B (protein stain) for 30 minutes. Cells were then washed with 0.1% acetic acid, air dried, and the bound sulfurhodamine B was dissolved with 10 mmol/L unbuffered Tris-base (pH 10.5). The plates were read in a microplate reader (A_{564}) and synergy was determined using CalcuSyn software, which calculates the combination index based on the percent cell survival at varying doses of the drug treatments, both alone and in combination. A combination index greater than 1 indicates antagonism, equal to 1 is additivity, and less than 1 is synergism.

Results

Lonafarnib treatment alters microtubule structure

To examine the effects of lonafarnib on interphase microtubules, we performed live cell microtubule imaging using MCF-7 breast cancer cells stably expressing GFP:α -tubulin. This cell line allows for the visualization of microtubules in living cells and eliminates the possibility of artifacts associated with fixed tissue analyses. Cells were treated for 48 hours with 5 and 10 − mol/L lonafarnib (mean 72-hour IC_{50} of lonafarnib was 8 − mol/L in seven cancer cell lines tested; data not shown) and microtubules were observed using live-cell epifluorescence microscopy (Fig. 1*A*). Nearly all untreated control cells observed had an extensive, fine, and organized microtubule network. In contrast, lonafarnib treatment led to a dose-dependent increase in microtubule bundling compared with control cells ($P < 0.05$; Fig. 1*B*). Treatment with 5 and 10 − mol/L lonafarnib led to nearly 10% and 25% of cells harboring extensive microtubule bundling, respectively. Similar microtubule bundles were observed in nearly 60% of cells treated with paclitaxel, whereas cells treated under the same condition with the non-microtubule targeting, DNA-intercalating agent Adriamycin had identical microtubule morphologies as control cells.

To examine whether these effects were cell line specific, we performed immunofluorescence microscopy with an anti α -tubulin antibody on A549 and H1299 human lung cancer cells treated with lonafarnib. Representative data from this experiment are shown in Supplementary Fig. S1-*A* depicting a dose-dependent increase in microtubule bundling following lonafarnib treatment for 48 hours.

Lonafarnib treatment increases tubulin acetylation and microtubule stability

The appearance of microtubule bundles after lonafarnib treatment in A549, H1299, and MCF-7 cells raises the possibility that lonafarnib can affect microtubule stability in a manner similar to paclitaxel. To validate this hypothesis, indirect immunofluorescence using an antibody against acetylatedα -tubulin was done. Acetylation of α -tubulin at lysine 40 is an established

marker of microtubule stability (36). Thus, the amount of acetylated tubulin is thought to be proportional to the stability of the microtubule. As shown in Fig. 1*C*, lonafarnib treatment for 48 hours resulted in a marked dose-dependent increase in acetylated α -tubulin, in contrast to the low basal levels of acetylated tubulin in untreated cells. This effect was similar to paclitaxel-induced tubulin acetylation, suggesting that lonafarnib may also affect microtubule stability similar to paclitaxel.

To further probe the effects of lonafarnib treatment on microtubule stabilization, a cell-based tubulin polymerization assay was done (32,33). This quantitative tubulin polymerization assay is based on the fact that drug-stabilized microtubule polymers remain detergent insoluble when extracted in a hypotonic buffer and, therefore, remain in the pellet after centrifugation. Conversely, the pool of soluble tubulin dimers remains in the supernatant. Lonafarnib treatment resulted in a dose-dependent increase in tubulin polymerization, as shown by the increase in the percentage of tubulin found in the pellet fraction, as compared with untreated control cells (Fig. 1*D*). Specifically, untreated cells contain almost no stabilized tubulin (0% tubulin in the pellet) under our experimental conditions, whereas lonafarnib treatment (5-20 − mol/L) led to a dose-dependent increase in tubulin polymerization (25-60% of total tubulin in the pellet fraction). Similarly, treatment with 5 nmol/L paclitaxel resulted in about 80% tubulin polymerization. The same blot was reprobed with an antibody against acetylated α -tubulin. A similar dose-dependent increase in acetylated α -tubulin in the pellet was observed on lonafarnib treatment and this shift of acetylated-tubulin towards the polymerized fraction was greater than total tubulin. Thus, the majority of tubulin polymers in the pellet fraction represent stabilized acetylated microtubules rather than random microtubules trapped in this fraction.

Transmission electron microscopy confirms microtubule bundles in lonafarnib-treated cells

To obtain high-resolution analysis of lonafarnib-induced changes of the microtubule architecture, we did transmission electron microscopy (34). In contrast to control cells, which had individual microtubules throughout the cell cytoplasm, lonafarnib treatment induced the formation of microtubule bundles, similar to the bundles observed with paclitaxel (Supplementary Fig. S2-*B*). Interestingly, lonafarnib treatment mainly led to the formation of loose microtubule clusters that were longer in length but not as tightly packed as paclitaxel-induced microtubule bundles, suggesting that lonafar-nib-induced bundles may differ morphologically from paclitaxel-induced bundles (Supplementary Fig. S2-*B, insets*).

Lonafarnib suppresses microtubule dynamics in MCF-7 cells

Drugs that target microtubules potently suppress microtu-bule dynamics at relatively low concentrations (16,34) and this function is essential for their activity. Our results show lonafarnib targets cellular microtubules; therefore, we investigated whether lonafarnib also affects microtubule dynamics, similar to other microtubule-targeting drugs. To test this hypothesis, we measured microtubule dynamics in living MCF7-GFP:tubulin breast cancer cells using live-cell fluorescence microscopy. Time-lapse sequences of microtubule movements were generated from untreated and lonafarnib-treated cells. Representative time frames show micro-tubule growth (*white arrows*), shortening (*black arrows*), and pause (*white dashed arrows*) in untreated control cells (Fig. 2*A*). To quantitate the effects of lonafarnib on microtubule dynamics, we tracked microtubule movements in cells treated with 10 − mol/L lonafarnib and untreated control cells. Individual microtubule life history plots, depicting changes in microtubule length over time, were generated (Fig. 2*B*).

From these life history plots various variables of microtubule dynamics were measured, comparing the dynamicity of micro-tubules in control cells and lonafarnib-treated cells (Table 1). These data show that there is a significant difference ($P < 0.05$) in the mean rate (− m/min) of microtubule growth and shortening with a decrease of 31% and 41%, respectively, when

lonafarnib-treated cells (10 − mol/L for 48 hours) are compared with control cells. Consequently, mean growth and shortening length (− m) also decreased by 34% and 42%, respectively. When the percentage of total time that microtubules spent in growth, shortening, and pause states was determined, the growth time dropped from 30% to 17%, shortening time from 17% to 8.8%, and paused time increased from 53% to 74.2%; whereas the rescue and catastrophe frequencies per micrometer increased 31% and 12%, respectively (see Materials and Methods for definition). The overall dynamicity of microtubules, which represents the total tubulin length change per minute after lonafarnib (10 − mol/L) treatment, decreased by 63%. At 20 − mol/L lonafarnib, microtubules were almost completely stabilized and most cells had few, if any, dynamic microtubules.

Combination of lonafarnib with paclitaxel synergistically increases acetylated tubulin, mitotic arrest, and cell death

FTIs have been shown to synergize with microtubule stabilizing drugs in numerous preclinical models as well as in a phase I clinical trial (25). These observations were confirmed in our laboratory by performing combination index analysis assays of 10 different human cancer cell lines treated with paclitaxel and lonafarnib. These assays revealed a marked synergy (combination index = 0.2-0.7) between the two drugs (data not shown) and is consistent with previous findings. Our results, together with the reported literature, prompted us to hypothesize that the synergy of lonafarnib with taxanes may in part be due to their combined effects on cellular microtubule acetylation and stability.

To test this hypothesis, we quantitated acetylated tubulin levels using flow cytometry in cells treated for 16 hours (unlike the 48-hour treatment in Fig. 1*B*) with lonafarnib and paclitaxel, both alone and in combination. As shown in Fig. 4*A*, there was not a significant difference in acetylated tubulin levels between control untreated cells and cells treated for only 16 hours with lonafarnib (1, 5, and 10 − mol/L) or paclitaxel (2, 5, and 10 nmol/L) alone. In contrast, the combination of 1, 5, and 10 − mol/L lonafarnib with as low as 2 nmol/L paclitaxel resulted in a marked increase of acetylated tubulin similar to that observed with 100 nmol/L of paclitaxel alone (Fig. 3*A*). Notably, non-microtubule-targeting chemotherapy drugs, such as Adriamycin (DNA-intercalating antibiotic) and U89 (antimetabolite), had no effect on acetylated tubulin levels, whereas the microtubule-destabilizing drug vincris-tine led to a slight decrease of acetylated tubulin levels compared with untreated cells (Fig. 3*A*).

To further explore the synergistic combination of lonafarnib with paclitaxel, immunofluorescence analysis of acetylated tubulin at two different time points was done (Fig. 3*B*). This analysis confirmed the marked increase in acetylated tubulin levels after 16 hours when low doses of lonafarnib (at 0.5, 1, and 5 − mol/L) were combined with low doses of 2 nmol/L paclitaxel. At 32 hours of treatment, similar effects on acetylated tubulin were observed, suggesting that this effect is maintained for at least 32 hours.

Because tubulin acetylation is associated with microtubule stability, we examined whether the increased levels of acetylated tubulin observed with the combination of lonafarnib and paclitaxel resulted in increased mitotic arrest and cell death. Flow cytometry analysis of DNA content revealed that the combination of lonafarnib and paclitaxel led to a synergistic increase in G_2-M arrest as compared with each drug alone (Fig. 3*C*). Specifically, 16-hour treatment with as low as 0.5 − mol/L lonafarnib + 2 nmol/L paclitaxel resulted in a dramatic increase in G_2-M arrested cells as compared with untreated cells or cells treated with each drug alone. Longer treatment (32 hours) with the same drug combinations resulted in a dose-dependent increase in apoptotic cell death that is likely due to cells previously arrested in mitosis becoming apoptotic (Fig. 3*C*). The percentage of apoptotic cells in the combination treatments was similar to that achieved with paclitaxel at 100 nmol/L, whereas either drug alone at low dose produced minimal apoptotic cells. Overall, these results show that the lonafarnib/paclitaxel-mediated

increase in tubulin acetylation correlates with a synergistic increase in mitotic arrest and cell death.

The synergistic increase in tubulin acetylation correlates with farnesyl transferase inhibition

Because lonafarnib inhibits the FT enzyme, we wanted to determine if the increase in tubulin acetylation observed with the combination of lonafarnib and paclitaxel correlates with FT inhibition in cells. If so, it would suggest that the observed increase in tubulin acetylation may be a consequence of FTase inhibition. To do this, HDJ-2 was used as a readout for FT inhibition, since FTI treatment inhibits HDJ-2 farnesylation resulting in the appearance of a slower-migrating non-farnesylated HDJ-2 form. As shown in Fig. 4*A*, 1 − mol/L lonafarnib alone and in combination with paclitaxel inhibited HDJ-2 farnesylation in a time-dependent manner, as assessed by the increase of the non-farnesylated (upper band) and concomitant decrease of the farnesylated HDJ-2 band (lower band). As expected, paclitaxel alone had no effect on HDJ-2 farnesylation. When the same blots were reprobed for acetylated α -tubulin, we observed a correlation between inhibition of HDJ-2 farnesylation and tubulin acetylation beginning at 3 hours of treatment with the lonafarnib/paclitaxel combination. In contrast, minimal effect on tubulin acetylation was observed with either drug alone. Taken together, these results show a positive temporal correlation between FT inhibition and tubulin acetylation when lonafarnib and paclitaxel are combined.

Next, we wanted to determine if there is also a correlation between tubulin acetylation and mitotic arrest. Therefore, in parallel with the time course experiment described above, we quantitated the percentage of cells in mitosis after treatment with the combination of lonafarnib and paclitaxel. This result is represented in Fig. 4*B* showing that there is about a 3-hour delay between the increase in microtubule acetylation (starting at 3 hours) and the first indication of mitotic arrest (at 6 hours). Furthermore, the percentage of cells in mitosis increased with longer exposures to the combination of the two drugs, peaking at 12 hours of treatment. Overall, this result shows that when lonafarnib and paclitaxel are combined, microtubule acetylation occurs before mitotic arrest and suggests that there is a correlation between tubulin acetylation/stability and mitotic arrest.

Lonafarnib in combination with paclitaxel inhibits the tubulin deacetylating activity of histone deacetylase 6

Our observation that lonafarnib and paclitaxel synergistically enhance tubulin acetylation (Fig. 3) prompted us to explore the possibility that this effect is due to the functional inhibition of the only known tubulin-specific deacetylase (30), HDAC6. To determine the effect of lonafarnib on HDAC6 function, we transfected A549 cells with FLAG-tagged HDAC6 (wild-type or catalytic subunit mutant) and these proteins were immunoprecipitated with an anti-FLAG antibody (see Materials and Methods). The tubulin deacetylase activity of HDAC6 in the presence of lonafarnib and paclitaxel was assayed *in vitro* by coincubating the immunoprecipitants with purified bovine brain microtubule protein. Western blot analyses of acetylated tubulin levels were used as a read-out for HDAC6 activity (Fig. 5*A*), such that HDAC6 functionality is evidenced by tubulin deacetylation. As a positive control, we used trichostatin A, which inhibits the function of all histone deacetylases including HDAC6. As expected, bovine brain tubulin is heavily acetylated (*lane 1*) and coincubation with wt-HDAC6 almost completely deacetylated tubulin (*lane 3*). In contrast, coincubation with the catalytically inactive mutant HDAC6 had no effect on tubulin acetylation (*last lane*). The addition of lonafarnib or paclitaxel alone to the purified wild-type HDAC6-tubulin complex had no effect on HDAC6 activity because tubulin was heavily deacetylated, indicating normal HDAC6 activity. In contrast, when lonafarnib (variable doses) and paclitaxel (kept constant at 10 − mol/L) were combined *in vitro*, there was a dose-dependent increase of tubulin acetylation, suggesting that the combination of these agents inhibits tubulin deacetylating HDAC6 activity.

Paclitaxel alone had no effect on HDAC6 activity even at 100 − mol/L. We also tested the microtubule depolymerizing agent colchicine for HDAC6 inhibitory activity, and like paclitaxel, it did not inhibit HDAC6 function.

Since our results suggest that the combination of lonafarnib and paclitaxel synergistically inhibits HDAC6 function, we wanted to determine if these drugs also affect the function of other histone deacetylases. Thus, we treated A549 cells with lonafarnib, alone and in combination with paclitaxel, for 16 hours and probed for acetylated histone 3. Trichostatin A (a pan-HDAC inhibitor) was included as a positive control. As expected, treatment with trichostatin A resulted in increased levels of acetylated histone 3. In contrast, no effect on acetylated histone 3 was observed with lonafarnib treatment either alone or in combination with paclitaxel (Supplementary Fig. S2), suggesting that lonafarnib and/or paclitaxel does not affect the function of other histone deacetylases.

To probe the importance of HDAC6 inhibition in the mechanism of synergy between lonafarnib and paclitaxel, we combined a specific HDAC6 inhibitor, tubacin, with paclitaxel. This experiment allows us to determine whether the combination of a specific HDAC6 inhibitor with paclitaxel leads to a synergistic increase in tubulin acetylation, similar to the lonafarnib/paclitaxel combination. Western blot analysis of A549 cells treated with the combination of tubacin and paclitaxel at low doses (beginning at 0.3 − mol/L tubacin and 1 nmol/L paclitaxel) led to a synergistic increase in acetylated tubulin, as compared with either drug alone (Fig. 5*B*). These findings were confirmed with acetylated tubulin immunofluorescence (data not shown). Thus, specific inhibition of HDAC6 (e.g., with tubacin) in combination with paclitaxel leads to a synergistic increase in acetylated tubulin, further suggesting that the lonafarnib/paclitaxel inhibition of HDAC6 activity provides a mechanistic basis for the enhanced tubulin acetylation. Furthermore, the addition of 3 and 10 − mol/L tubacin (IC_{50} > 1 mmol/L) to paclitaxel (IC_{50} 7.7 ± 1.7 − mol/L) decreased the IC_{50} of paclitaxel, 20.8% and 31.5%, respectively (Supplementary Table S1). Similar results were also observed when tubacin was combined with docetaxel (Supplementary Table S1), suggesting that although tubacin as a single agent is not cytotoxic, its affect on tubulin acetylation can enhance the cytotoxicity of paclitaxel.

To further explore the functional importance of HDAC6 in the synergy between lonafarnib and paclitaxel, we tested this drug combination in a pair of cell lines engineered to stably express either wild-type H DAC6 (HDAC6-wt) or a catalytic mutant HDAC6 (HDAC6-mut). These cells lines will allow us to determine if a functional HDAC6 protein is required for the observed effects on acetylated tubulin. In agreement with previously published data (30), HDAC6-wt cells had lower baseline levels of acetylated tubulin relative to HDAC6-mut cells, consistent with the presence of a functional versus a nonfunctional HDAC6 (Fig. 5*C*, untreated). Upon treatment with the lonafarnib/paclitaxel combination, there was a synergistic increase in acetylated tubulin in HDAC6-wt cells as expected; however, the lonafarnib/paclitaxel combination had no effect on tubulin acetylation in the HDAC6-mut cells. These results indicate that the synergistic increase in acetylated tubulin induced by the lonafarnib/paclitaxel combination is dependent on the presence of a functional HDAC6.

Next, we wanted to determine if functional HDAC6 is required not only for the synergistic increase in acetylated tubulin with the lonafarnib/taxane combination (Fig. 5*C*) but also for the synergistic antiproliferative activity of the drugs. Thus, we did cytotoxicity assays employing the routinely used combination index analysis to assess synergy between the two drugs against cells with HDAC6-wt and HDAC6-mut genetic background. Our results show that the combination of lonafarnib with docetaxel resulted in a robust synergistic antiproliferative effect in HDAC6-wt cells (mean combination index = 0.4, indicating strong synergy; Fig. 5*D*). In stark contrast, the combination of lonafarnib and docetaxel was antagonistic in the HDAC6-

mut cells (mean combination index = 2.5), suggesting that the lack of functional HDAC6 in these cells not only precludes increased levels of acetylated tubulin with this drug combination but also abolishes their antiproliferative synergy. To confirm that the combination of docetaxel with lonafarnib inhibits the tubulin deacetylase activity of HDAC6 *in vitro*, similar to our previous results with paclitaxel (Fig. 5*A*), we used cells stably expressing wild-type HDAC6 to immunoprecipitate HDAC6, and performed an *in vitro* tubulin deacetylase assay. Our data show that the combination of 10 − mol/L lonafarnib with 10− mol/L docetaxel resulted in a synergistic inhibition of HDAC6 function, as evidenced by the appearance of acetylated tubulin, whereas either drug alone had no effect on HDAC6 functionality (Fig. 5*E*). Collectively, these data provide a mechanistic link between HDAC6 inhibition, tubulin acetylation, and the synergistic interaction of these drugs.

Discussion

Analyzing the effects of lonafarnib as a single agent on microtubules

The FTIs were developed as targeted therapies against cancers with oncogenic Ras mutations, however, FTIs were shown to retain their activity independently of Ras status (11–13). Here we examined the effects of the FTI lonafarnib on interphase microtubules in human cancer cells. Our results show that prolonged exposure (48 hours) to lonafarnib alone leads to microtubule stabilization as evidenced by increased tubulin acetylation, suppression of microtubule dynamics, and bundle formation (Figs. 1 and 2;Table 1). Because tubulin acetylation is an established marker of microtubule stability (36), we believe that the lonafarnib-induced microtubule stabilization may contribute to its antiproliferative effects, similar to taxanes and epothilones. However, it is important to note that the microtubule-stabilizing capacity of lonafarnib is weak relative to other established microtubule stabilizing agents, which stabilize microtubules at low nanomolar concentrations. This suggests that the mechanism by which lonafarnib induces microtubule stabilization may differ from traditional microtubule-stabilizing agents (e.g., taxanes). Further supporting this hypothesis is our electron microscopy analysis (Supplementary Fig. S1-*B*), which shows that lonafarnib-induced microtubule bundles are longer and not as tightly clustered as paclitaxel-induced bundles, suggesting that their differing morphologies may stem from alternative mechanisms of bundle formation. Thus, we propose that lonafarnib is a microtubule-stabilizing agent; however, its mechanism of microtubule stabilization likely differs from that of established microtubule-stabilizing agents.

Microtubule acetylation and the mechanism of synergy between lonafarnib and taxanes

Previous reports have shown that FTIs synergize with taxanes and epothilones in a variety of human cancer cell lines *in vitro* and *in vivo* (22,24); however, the mechanism underlying this synergy is unknown. Our results show that the combination of low doses of lonafarnib (beginning at 0.5 − mol/L) and paclitaxel (2 nmol/L) resulted in a dramatic increase in tubulin acetylation (Fig. 3*A*-*C*) compared with untreated cells or each drug treatment alone. Importantly, the mean Cmax of lonafarnib achieved in patients dosed twice daily with 200 mg of lonafarnib is 4.4 − mol/L[6] and, therefore, the doses (lonafarnib beginning at 0.5 − mol/L) at which we observed synergistic enhancement of acetylated tubulin are within the Cmax. Furthermore, the effect of lonafarnib/paclitaxel on acetylated tubulin was observed in as little as 3 hours of drug treatment (Fig 4*A*) and preceded the synergistic increase in mitotic arrest (Figs. 3*C* and 4*B*), suggesting that increased microtubule acetylation/stability is associated with aberrant mitotic arrest and cell death. Nevertheless, it remains unclear if lonafarnib/paclitaxel-induced microtubule acetylation only serves as marker for cell death or instead is the catalyst, and therefore studies are under way addressing this issue.

[6]R. Bishop, unpublished data.

Mechanistically, we show that the synergistic increase in microtubule acetylation is due to the effect of the combination of lonafarnib and paclitaxel on HDAC6 (Fig. 5). We propose that the enhanced tubulin acetylation we observe is due to the inhibition of HDAC6 function. We provide four lines of evidence to support this claim. First, we show that the combination of lonafarnib and paclitaxel inhibits HDAC6 tubulin deacetylating activity *in vitro*, whereas either drug alone had no effect (Fig 5*A*). Second, we can reproduce the lonafarnib/paclitaxel-induced increase in tubulin acetylation by using tubacin, a specific HDAC6 inhibitor, in combination with paclitaxel (Fig. 5*B*). This suggests that pharmacologic inhibition of HDAC6 in combination with paclitaxel synergistically increases tubulin acetylation. Third, cells expressing a catalytically inactive HDAC6 (HDAC6-mt) fail to show an increase in acetylated tubulin when lonafarnib and paclitaxel are combined (Fig. 5*C*), suggesting that this drug combination requires functional HDAC6 to retain efficacy. Fourth, the robust cytotoxic synergy of lonafarnib and docetaxel is lost in these cells expressing mutant HDAC6, whereas potent synergy remains in their wild-type HDAC6 counterparts (Fig. 5*D*). This observation provides evidence that the deacetylating activity of HDAC6 is required for the lonafarnib/taxane synergy, providing a mechanistic link between functional HDAC6, tubulin acetylation, and cell death. However, it is still unknown whether the effect of the lonafarnib/taxane combination on HDAC6 function is due to direct binding of these drugs to this enzyme or due to their effects on microtubule stability, which in turns alters the affinity of HDAC6 for the microtubule. We favor the latter scenario because either drug alone does not alter HDAC6 function, reducing the likelihood that these drugs bind HDAC6 directly.

Is there a biological link between FTase inhibition and microtubule acetylation?

Because all FTIs tested to date synergize with paclitaxel, it is likely that they share a common mechanism of synergy related to FT inhibition. In Fig. 4*A*, we show that the increase in tubulin acetylation observed with the low dose lonafarnib/paclitaxel combination correlates with FT inhibition. This result suggests that inhibition of FT may be biologically linked with enhanced tubulin acetylation. Currently, there are no reports of a link between the FTase enzyme and interphase microtubules. Preliminary data from our laboratory in 50 human cancer cell lines used in the National Cancer Institute Anticancer Drug Screen (http://dtp.nci.nih.gov) have revealed that acetylated tubulin protein levels negatively correlated with FTase gene expression and protein levels (COMPARE analysis http://itbwork.nci.nih.gov/CompareServer/CompareServer;).[7] Thus, it may be possible that proteins regulating microtubule stability are farnesylated by FTase; consequently, inhibition of FTase by lonafarnib may in turn affect microtubule stability. In fact, it is already known that the mitotic microtubule-associated protein, CENP-E, is farnesylated and its association with microtubules during mitosis is altered in mitotic cells (27). Thus, further investigation of a putative link between FTase and interphase microtubules is warranted.

Overall, our data show that treatment with lonafarnib alone causes microtubule bundling, increased microtubule acetylation and stabilization, and suppression of microtubule dynamics. This result is consistent with lonafarnib being a microtubule-stabilizing agent, in addition to its role as an FTI. Importantly, our data also show that functional HDAC6 is required for the synergy between lonafarnib and taxanes and suggest that there is a link between FTase and tubulin acetylation. As there are ongoing phase II and III trials testing the efficacy of this drug combination, elucidating the molecular mechanism(s) of synergy can provide insight into the design of future combination cancer therapies.

[7]Unpublished data.

Supplementary Material

Refer to Web version on PubMed Central for supplementary material.

Acknowledgements

Grant support: NIH 1R01 CA100202 and Aventis Pharmaceuticals. BESCT grant no. DAMD17-01-1-0689 (to F.R. Khuri).

We thank Drs. Mary Ann Jordan and Kathy Kamath (University of California Santa Barbara, Santa Barbara, CA) for providing us with the MCF-7 cells stably expressing GFP:α -tubulin and for sharing their invaluable experience on performing the live-cell microtubule dynamic assays; Dr. Stuart Schreiber (Harvard University, Boston, MA) for providing us with tubacin and FLAG-HDAC6 constructs, and for providing guidance to Jason Wong (gm38627, awarded to Stuart L. Schreiber); Dr. W. Robert Bishop for his invaluable insight and for providing us with Lonafarnib (Schering-Plough Research Institute); Dr. Robert Apkarian, director of the electron microscopy core facility at Emory University, for his help with transmission electron microscopy; Cindy Giver for her help with flow cytometry; and the Winship Cancer Institute Cancer Imaging and Microscopy Core for their support and service.

References

1. Brunner TB, Hahn SM, Gupta AK, et al. Farnesyl-transferase inhibitors: an overview of the results of preclinical and clinical investigations. Cancer Res 2003;63:5656–68. [PubMed: 14522880]
2. Adjei AA. Blocking oncogenic Ras signaling for cancer therapy. J Natl Cancer Inst 2001;93:1062–74. [PubMed: 11459867]
3. Hahn SM, Bernhard E, McKenna WG. Farnesyltrans-ferase inhibitors. Semin Oncol 2001;28:86–93. [PubMed: 11706400]
4. McCormick F. Ras-related proteins in signal trans-duction and growth control. M ol Reprod Dev 1995;42:500–6.
5. Jackson JH, Cochrane CG, Bourne JR, et al. Farnesyl modification of Kirsten-ras exon 4B protein is essential for transformation. Proc Natl Acad Sci U S A 1990;87:3042–6. [PubMed: 2183224]
6. Kato K, Cox AD, Hisaka MM, et al. Isoprenoid addition to Ras protein is the critical modification for its membrane association and transforming activity. Proc Natl Acad Sci U S A 1992;89:6403–7. [PubMed: 1631135]
7. Willumsen BM, Christensen A, Hubbert NL, Papageorge AG, Lowy DR. The p21 ras C terminus is required for transformation and membrane association. Nature 1984;310:583–6. [PubMed: 6087162]
8. Barbacid M. Ras genes. Annu Rev Biochem 1987;56:779–827. [PubMed: 3304147]
9. Bos JL. Ras oncogenes in human cancer: a review. Cancer Res 1989;49:4682–9. [PubMed: 2547513]
10. Li T, Sparano JA. Inhibiting Ras signaling in the therapy of breast cancer. Clin Breast Cancer 2003;3:405–16. [PubMed: 12636885]discussion 17–20
11. End DW, Smets G, Todd AV, et al. Characterization of the antitumor effects of the selective farnesyl protein transferase inhibitor R115777 *in vivo* and *in vitro*. Cancer Res 2001;61:131–7. [PubMed: 11196150]
12. Nagasu T, Yoshimatsu K, Rowell C, Lewis MD, Garcia AM. Inhibition of human tumor xenograft growth by treatment with the farnesyl transferase inhibitor B956. Cancer Res 1995;55:5310–4. [PubMed: 7585593]
13. Sepp-Lorenzino L, Ma Z, Rands E, et al. A peptidomimetic inhibitor of farnesyl:protein transferase blocks the anchorage-dependent and -independent growth of human tumor cell lines. Cancer Res 1995;55:5302–9. [PubMed: 7585592]
14. Moasser MM, Rosen N. The use of molecular markers in farnesyltransferase inhibitor (FTI) therapy of breast cancer. Breast Cancer Res Treat 2002;73:135–44. [PubMed: 12088116]
15. Nogales E. Structural insights into microtubule function. Annu Rev Biochem 2000;69:277–302. [PubMed: 10966460]
16. Jordan MA. Mechanism of action of antitumor drugs that interact with microtubules and tubulin. Curr Med Chem Anti-Canc Agents 2002;2:1–17.
17. Jordan MA, Wilson L. Microtubules as a target for anticancer drugs. Nat Rev Cancer 2004;4:253–65. [PubMed: 15057285]

18. Drukman S, Kavallaris M. Microtubule alterations and resistance to tubulin-binding agents [review]. Int J Oncol 2002;21:621–8. [PubMed: 12168109]
19. Rowinsky EK. The development and clinical utility of the taxane class of antimicrotubule chemotherapy agents. Annu Rev Med 1997;48:353–74. [PubMed: 9046968]
20. Checchi PM, Nettles JH, Zhou J, Snyder JP, Joshi HC. Microtubule-interacting drugs for cancer treatment. Trends Pharmacol Sci 2003;24:361–5. [PubMed: 12871669]
21. Wartmann M, Altmann KH. The biology and medicinal chemistry of epothilones. Curr Med Chem Anti-Canc Agents 2002;2:123–48.
22. Moasser MM, Sepp-Lorenzino L, Kohl NE, et al. Farnesyl transferase inhibitors cause enhanced mitotic sensitivity to taxol and epothilones. Proc Natl Acad Sci U S A 1998;95:1369–74. [PubMed: 9465021]
23. Sun J, Blaskovich MA, Knowles D, et al. Antitumor efficacy of a novel class of non-thiol-containing peptidomimetic inhibitors of farnesyltransferase and geranylgeranyltransferase I: combination therapy with the cytotoxic agents cisplatin, Taxol, and gemcitabine. Cancer Res 1999;59:4919–26. [PubMed: 10519405]
24. Shi B, Yaremko B, Hajian G, et al. The farnesyl protein transferase inhibitor SCH66336 synergizes with taxanes *in vitro* and enhances their antitumor activity *in vivo*. Cancer Chemother Pharmacol 2000;46:387–93. [PubMed: 11127943]
25. Khuri FR, Glisson BS, Kim ES, et al. Phase I study of the farnesyltransferase inhibitor lonafarnib with paclitaxel in solid tumors. Clin Cancer Res 2004;10:2968–76. [PubMed: 15131032]
26. Crespo NC, Ohkanda J, Yen TJ, Hamilton AD, Sebti SM. The farnesyltransferase inhibitor, FTI-2153, blocks bipolar spindle formation and chromosome alignment and causes prometaphase accumulation during mitosis of human lung cancer cells. J Biol Chem 2001;276:16161–7. [PubMed: 11154688]
27. Crespo NC, Delarue F, Ohkanda J, et al. The farnesyltransferase inhibitor, FTI-2153, inhibits bipolar spindle formation during mitosis independently of transformation and Ras and p53 mutation status. Cell Death Differ 2002;9:702–9. [PubMed: 12058275]
28. Ashar HR, James L, Gray K, et al. Farnesyl transferase inhibitors block the farnesylation of CENP-E and CENP-F and alter the association of CENP-E with the microtubules. J Biol Chem 2000;275:30451–7. [PubMed: 10852915]
29. Taveras AG, Kirschmeier P, Baum CM. Sch-66336 (sarasar) and other benzocycloheptapyridyl farnesyl protein transferase inhibitors: discovery, biology and clinical observations. Curr Top Med Chem 2003;3:1103–14. [PubMed: 12769711]
30. Hubbert C, Guardiola A, Shao R, et al. HDAC6 is a microtubule-associated deacetylase. Nature 2002;417:455–8. [PubMed: 12024216]
31. Mabjeesh NJ, Escuin D, LaVallee TM, et al. 2ME2 inhibits tumor growth and angiogenesis by disrupting microtubules and dysregulating HIF. Cancer Cell 2003;3:363–75. [PubMed: 12726862]
32. Giannakakou P, Villalba L, Li H, Poruchynsky M, Fojo T. Combinations of paclitaxel and vinblastine and their effects on tubulin polymerization and cellular cytotoxicity: characterization of a synergistic schedule. Int J Cancer 1998;75:57–63. [PubMed: 9426691]
33. Giannakakou P, Sackett DL, Kang YK, et al. Paclitaxel-resistant human ovarian cancer cells have mutant β -tubulins that exhibit impaired pacli-taxel-driven polymerization. J Biol Chem 1997;272:17118–25. [PubMed: 9202030]
34. Vanier MT, Neuville P, Michalik L, Launay JF. Expression of specific tau exons in normal and tumoral pancreatic acinar cells. J Cell Sci 1998;111:1419–32. [PubMed: 9570759]
35. Kamath K, Jordan MA. Suppression of microtubule dynamics by epothilone B is associated with mitotic arrest. Cancer Res 2003;63:6026–31. [PubMed: 14522931]
36. Piperno G, LeDizet M, Chang XJ. Microtubules containing acetylated α -tubulin in mammalian cells in culture. J Cell Biol 1987;104:289–302. [PubMed: 2879846]

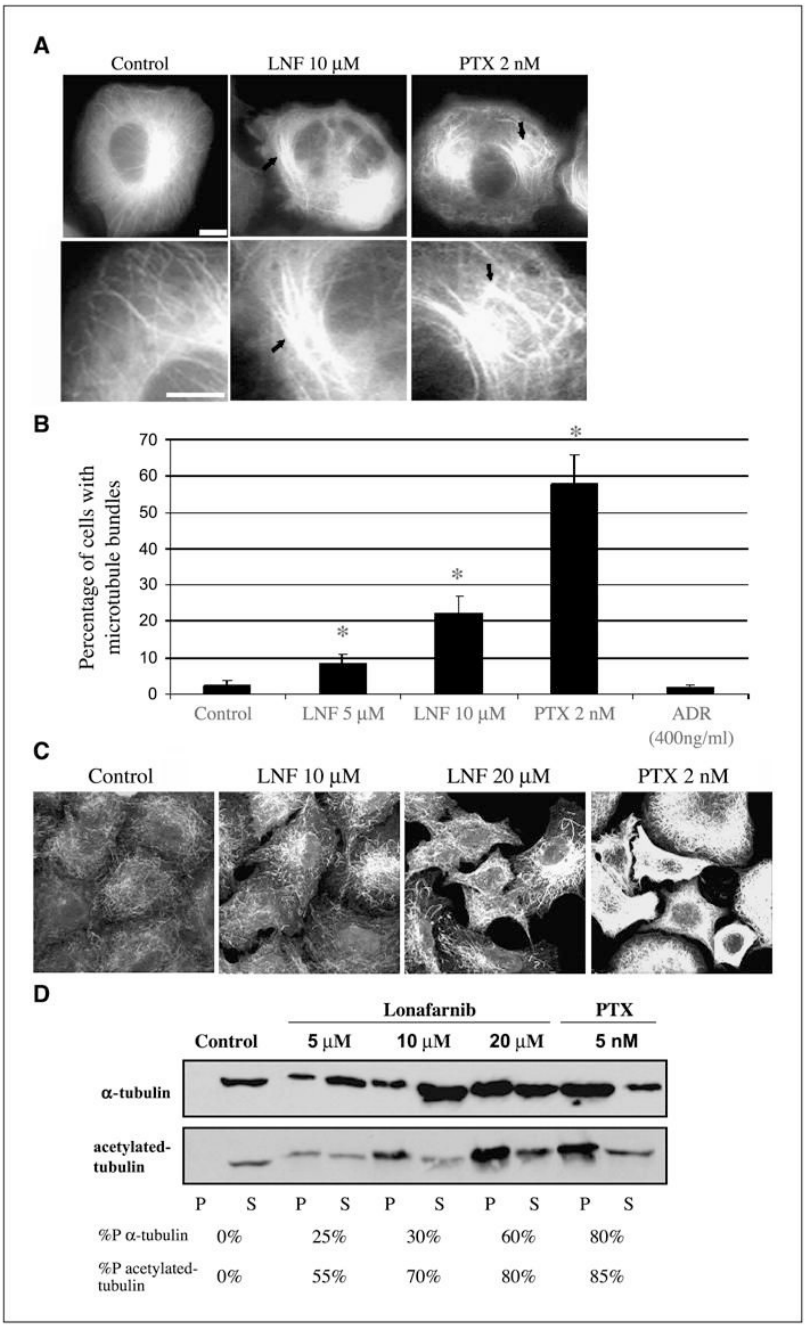

Figure 1.

Lonafarnib treatment alters microtubule structure and increases tubulin acetylation. *A*, MCF-7 breast cancer cells stably expressing GFP: α -tubulin were observed using live-cell fluorescence microscopy following the indicated drug treatments for 48 hours. *Solid arrows*, microtubule bundling. Bottom row displays higher magnification of microtubules shown in the top row. Bar, 10 − m. *B*, number of cells containing microtubule bundles following drug treatments shown in *A*. Asterisks denote a significant difference in the percentage of cells having microtubule bundles compared with control ($P < 0.05$). *Bars*, ±SD. *C*, A549 cells were treated with lonafarnib (*LNF*) for 48 hours and microtubules were visualized by immunofluorescence labeling using an antibody against acetylated α -tubulin. Treatment with paclitaxel (*PTX*) is

included as a positive control. Bar, 10 − m. *D*, Western blot analysis against total α -tubulin (*top*) and acetylated tubulin (*bottom*) on the polymerized (*P*) and soluble (*S*) fractions of protein lysates from A549 cells treated with the indicated drug concentrations for 48 hours. *%P*, relative percentage of polymerized tubulin for each drug treatment.

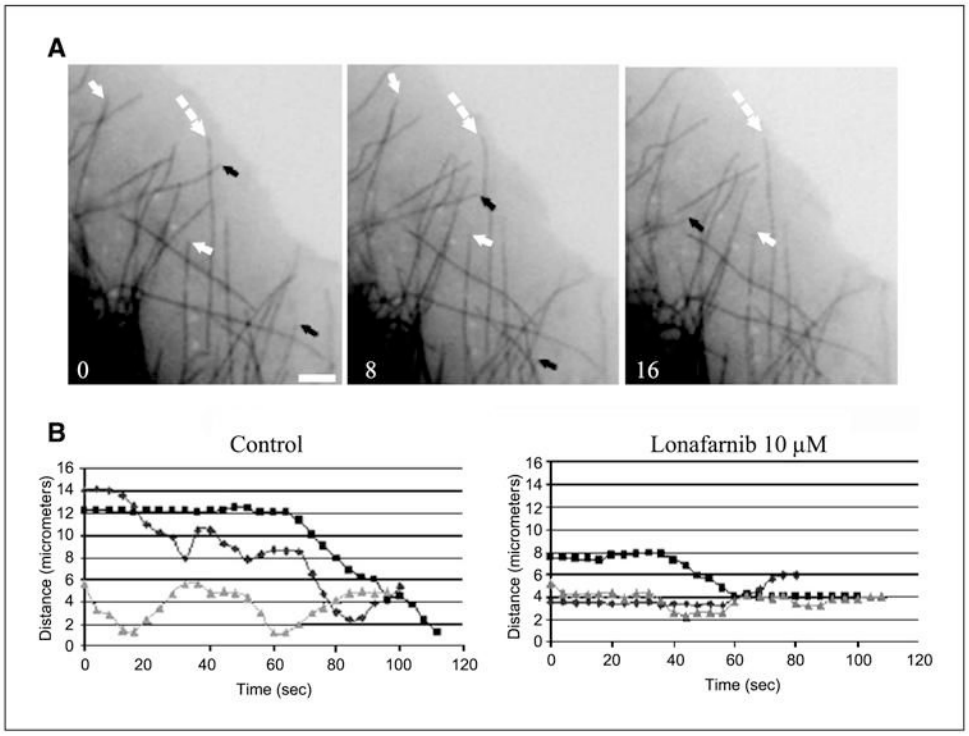

Figure 2.

Lonafarnib treatment suppresses microtubule dynamics in living MCF-7 cells. *A*, time lapse sequences of microtubules in untreated living MCF-7 cells stably expressing GFP: α -tubulin. Arrows depict dynamic microtubules that change length over the course of 16 seconds: *black arrows*, microtubule shortening; *white arrows*, microtubule growth; *dashed arrows*, paused microtubules. Bar, 5 − m. *B*, individual microtubule life history plots from control untreated cells or cells treated with 10 − mol/L lonafarnib for 48 hours. Growth events are seen as an increase in distance from a fixed point (*y axis*) over time (*x axis*) and shortening events show a decrease in distance over time.

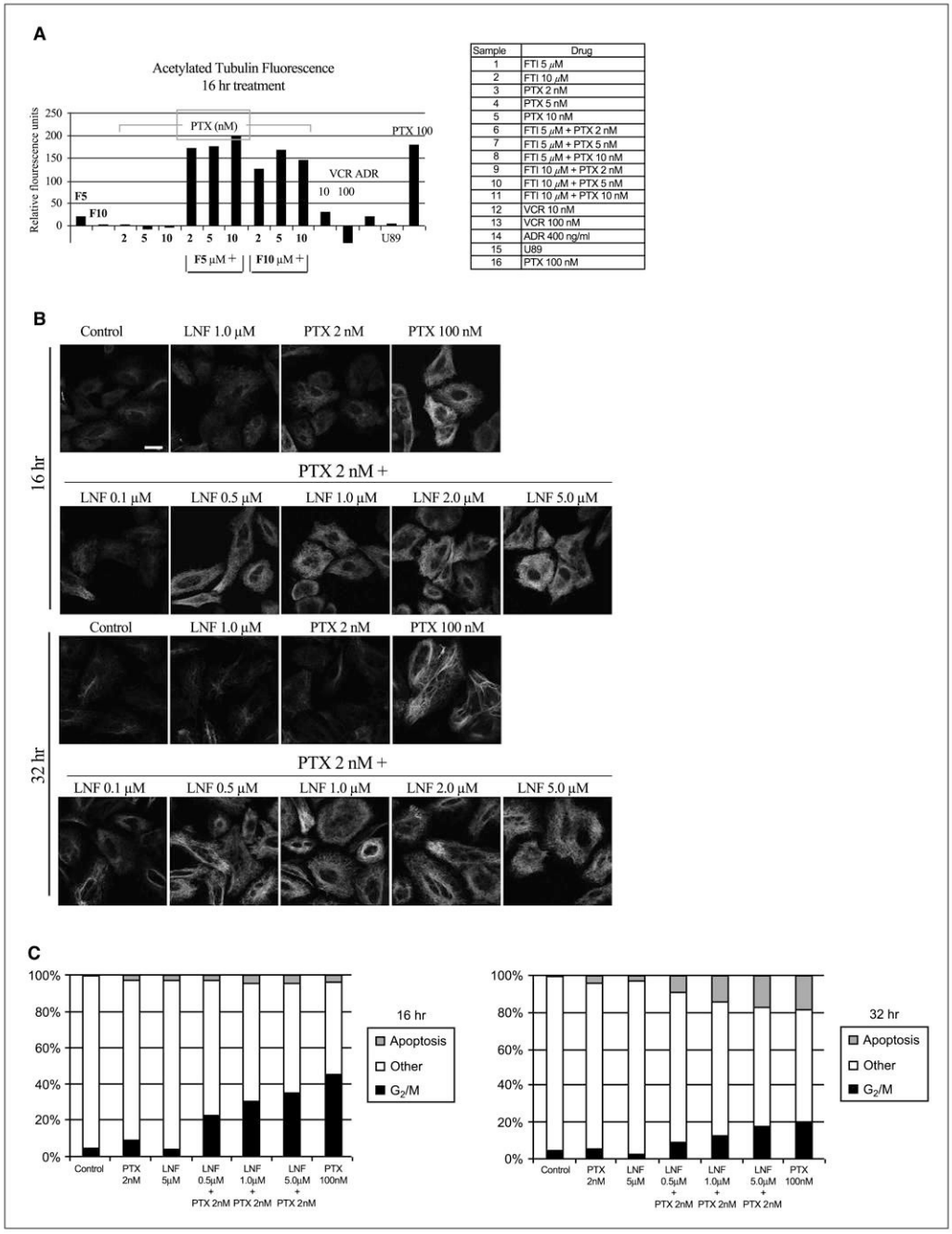

Figure 3.

Lonafarnib and paclitaxel synergistically increase acetylated tubulin, mitotic arrest, and apoptosis. *A*, flow cytometry was done with an acetylated tubulin antibody in A549 cells treated with the indicated drugs. Representation of acetylated tubulin levels after 16 hours of drug treatment. *Columns*, mean fluorescence for acetylated tubulin relative to that of control untreated cells (FTI: lonafarnib). *B*, acetylated tubulin immunofluorescence of cells treated with lonafarnib and paclitaxel, both alone and in combination, for 16 and 32 hours. *C*, cell cycle analysis for 16 and 32 hours of treatment with the combination of lonafarnib and paclitaxel.

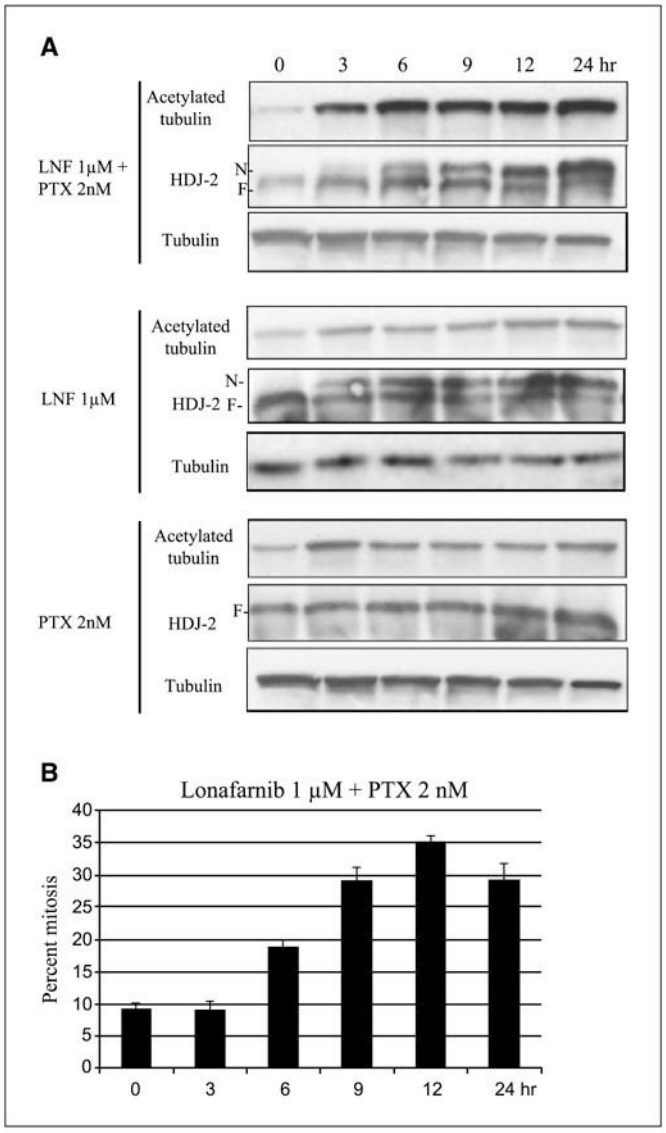

Figure 4.

The synergistic increase in acetylated tubulin caused by lonafarnib and paclitaxel treatment correlates with FT inhibition and mitotic arrest. *A*, Western blot analysis for acetylated tubulin, HDJ-2 (*N*, non-farnesylated band; *F*, farnesylated band), and total tubulin following lonafarnib and/or paclitaxel treatment over time. *B*, percent mitosis assessed by DNA staining, done in parallel and with the same drug treatments over time as in *A. Bars*, SD.

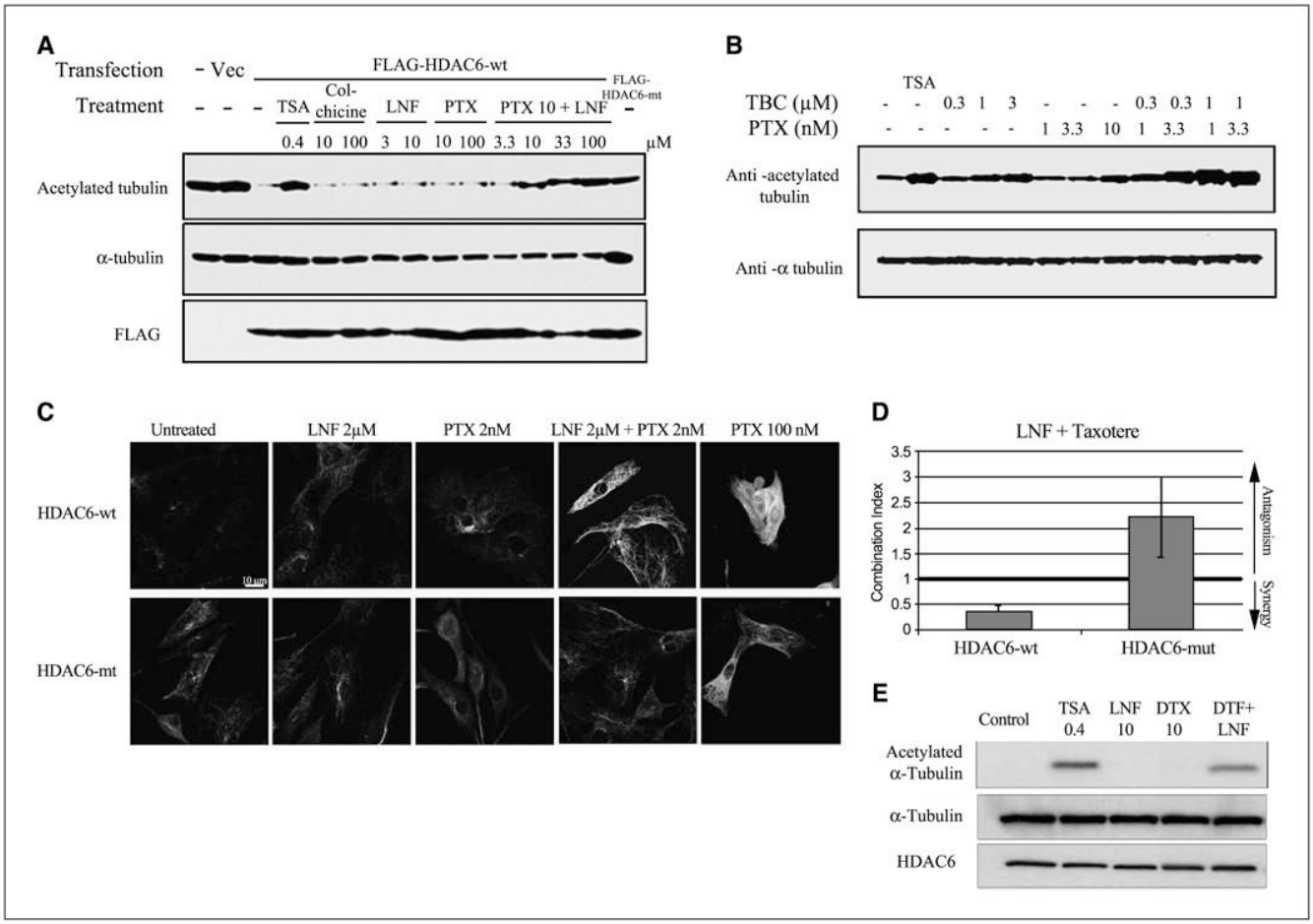

Figure 5.

The synergistic combination of lonafarnib and taxane prevents HDAC6 tubulin deacetylation *in vitro* and is dependent on HDAC6 functionality. *A*, representative Western blots of acetylated α -tubulin, total tubulin, and Flag, following immunoprecipitation (IP) from A549 cells transfected with either Flag-HDAC6-WT or Flag-HDAC6-mut. Before Western blotting the Flag-IP complexes were incubated *in vitro* with preassembled purified bovine brain microtubule protein in the presence of various drugs to determine the tubulin deacetylase activity of HDAC6 (*left-hand blot*). *B*, Western blotting of acetylated tubulin after treatment with tubacin, a specific HDAC6 inhibitor, both alone and in combination with paclitaxel. Trichostatin A (*TSA*) was used as additional positive control for pan-HDAC inhibition. As a control for total tubulin levels, blots were reprobed for α -tubulin. *C*, immunofluorescence analyses of acetylated tubulin in NIH-3T3 cells stably expressing either HDAC6-wt or HDAC-mut, following 16-hour drug treatments as indicated. *D*, assessment of synergy between lonafarnib and docetaxel in HDAC6-wt and HDAC6-mut using combination index analysis. The lonafarnib/docetaxel combination is synergistic in HDAC6-wt (combination index < 1) but is antagonistic in HDAC6-mt cells (combination index > 1). *Bars*, SD. *E*, representative Western blots of acetylated α -tubulin, total tubulin, and HDAC6 following immunoprecipitation (IP) from NIH-3T3 cells stably expressing Flag-HDAC6-WT. Before Western blotting the Flag-IP complexes were incubated *in vitro* with preassembled purified bovine brain microtubule protein in the presence of various drugs to determine the tubulin deacetylase activity of HDAC6. The *in vitro* effects of trichostatin A (pan-HDAC inhibitor), lonafarnib, and docetaxel (*DTX*) on acetylated α -tubulin are shown.

Table 1

Analysis of *in vivo* microtubule dynamics in the presence and absence of lonafarnib

Parameter	Control	Lonafarnib 10 − mol/L	Percent change
Growth			
Rate (− m/min)	11.2 ± 2.1	**7.7 ± 3.8**	−31%
Length (− m)	2.9 ± 1.6	**1.9 ± 0.9**	−34%
Time (min)	0.3 ± 0.08	0.28 ± 0.07	−7%
Shortening			
Rate (− m/min)	17.1 ± 4.0	**9.9 ± 3.3**	−41%
Length (− m)	5.3 ± 1.9	**3.1 ± 1.6**	−42%
Time (min)	0.34 ± 0.11	0.33 ± 0.1	−3%
Pause			
Time (min)	0.36 ± 0.23	0.40 ± 0.2	−11%
Percentage time spent			
Growth	30	**17**	
Shortening	17	**8.8**	
Pause	53	**74.2**	
Dynamicity (− m/min)	8.1 ± 4.0	**3.0 ± 1.9**	−63%
Rescue frequency (events/min)	4.1 ± 2.6	4.0 ± 2.5	−2%
Catastrophe frequency (events/min)	0.9 ± 0.8	0.88 ± 0.75	−2%
Rescue frequency (events/− m)	0.19 ± 0.15	**0.25 ± 0.21**	31%
Catastrophe frequency (events/− m)	0.33 ± 0.29	0.37 ± 0.31	12%
Number of cells	21	23	
Number of microtubules	81	69	

NOTE: Values in boldface differ significantly from control values at >99% confidence interval as determined by Student'*st* test. Values are mean ± SD.